A Simple Radionuclide-Driven Single-Ion Source

A. Piepke – University of Alabama
et al.

Citation of published version:

Montero Diez, M., et al. (2010): A Simple Radionuclide-Driven Single-Ion Source. *Review of Scientific Instruments,* 81(11).
DOI: https://doi.org/10.1063/1.3499505

A simple radionuclide-driven single-ion source

Cite as: Rev. Sci. Instrum. **81**, 113301 (2010); https://doi.org/10.1063/1.3499505
Submitted: 18 August 2010 . Accepted: 16 September 2010 . Published Online: 02 November 2010

M. Montero Díez, K. Twelker, W. Fairbank, G. Gratta, P. S. Barbeau, K. Barry, R. DeVoe, M. J. Dolinski, M. Green, F. LePort, A. R. Müller, R. Neilson, K. O'Sullivan, N. Ackerman, B. Aharmin, M. Auger, C. Benitez-Medina, M. Breidenbach, A. Burenkov, S. Cook, T. Daniels, K. Donato, J. Farine, G. Giroux, R. Gornea, K. Graham, C. Hagemann, C. Hall, K. Hall, D. Hallman, C. Hargrove, S. Herrin, A. Karelin, L. J. Kaufman, A. Kuchenkov, K. Kumar, J. Lacey, D. S. Leonard, D. Mackay, R. MacLellan, B. Mong, E. Niner, A. Odian, A. Piepke, A. Pocar, C. Y. Prescott, K. Pushkin, E. Rollin, P. C. Rowson, D. Sinclair, S. Slutsky, V. Stekhanov, J.-L. Vuilleumier, U. Wichoski, J. Wodin, L. Yang, and Y.-R. Yen

A simple radionuclide-driven single-ion source

M. Montero Díez,[1] K. Twelker,[1] W. Fairbank, Jr.,[2] G. Gratta,[1] P. S. Barbeau,[1] K. Barry,[1] R. DeVoe,[1] M. J. Dolinski,[1] M. Green,[1] F. LePort,[1] A. R. Müller,[1] R. Neilson,[1] K. O'Sullivan,[1] N. Ackerman,[3] B. Aharmin,[4] M. Auger,[5] C. Benitez-Medina,[2] M. Breidenbach,[3] A. Burenkov,[6] S. Cook,[2] T. Daniels,[7] K. Donato,[4] J. Farine,[4] G. Giroux,[5] R. Gornea,[5] K. Graham,[8] C. Hagemann,[8] C. Hall,[9] K. Hall,[2] D. Hallman,[4] C. Hargrove,[8] S. Herrin,[3] A. Karelin,[6] L. J. Kaufman,[9,a)] A. Kuchenkov,[6] K. Kumar,[7] J. Lacey,[8] D. S. Leonard,[9,b)] D. Mackay,[3] R. MacLellan,[10] B. Mong,[2] E. Niner,[10] A. Odian,[3] A. Piepke,[10] A. Pocar,[7] C. Y. Prescott,[3] K. Pushkin,[10] E. Rollin,[8] P. C. Rowson,[3] D. Sinclair,[11] S. Slutsky,[9] V. Stekhanov,[6] J.-L. Vuilleumier,[5] U. Wichoski,[4] J. Wodin,[3] L. Yang,[3] and Y.-R. Yen[9]

[1]*Department of Physics, Stanford University, Stanford, California 94305, USA*
[2]*Department of Physics, Colorado State University, Fort Collins, Colorado 80523, USA*
[3]*SLAC National Accelerator Laboratory, Menlo Park, California 94025, USA*
[4]*Department of Physics, Laurentian University, Sudbury, Ontario, Canada*
[5]*LHEP, Physikalisches Institut, University of Bern, Bern, Switzerland*
[6]*Institute for Theoretical and Experimental Physics, Moscow, Russia*
[7]*Department of Physics, University of Massachusetts, Amherst, Massachusetts 01003, USA*
[8]*Department of Physics, Carleton University, Ottawa, Ontario, Canada*
[9]*Department of Physics, University of Maryland, College Park, Maryland 20742, USA*
[10]*Department of Physics and Astronomy,University of Alabama, Tuscaloosa, Alabama 35487, USA*
[11]*Department of Physics, Carleton University, Ottawa and TRIUMF, Vancouver, Canada*

(Received 18 August 2010; accepted 16 September 2010; published online 2 November 2010)

We describe a source capable of producing single barium ions through nuclear recoils in radioactive decay. The source is fabricated by electroplating ^{148}Gd onto a silicon α-particle detector and vapor depositing a layer of BaF_2 over it. ^{144}Sm recoils from the alpha decay of ^{148}Gd are used to dislodge Ba^+ ions from the BaF_2 layer and emit them in the surrounding environment. The simultaneous detection of an α particle in the substrate detector allows for tagging of the nuclear decay and of the Ba^+ emission. The source is simple, durable, and can be manipulated and used in different environments. We discuss the fabrication process, which can be easily adapted to emit most other chemical species, and the performance of the source. © *2010 American Institute of Physics.* [doi:10.1063/1.3499505]

I. INTRODUCTION

It is often necessary in experimental settings to produce specific ionic species in a controlled manner. Indeed a large number of techniques to produce ions have been documented, from the early Penning sources to laser and electron-beam produced plasmas to thermal ionization.[1,2] These sources, however, can only operate under vacuum, and in many cases require expensive and complex infrastructure to allow for ion separation and delivery.

The work discussed here arises from the need to develop a simple source of monoatomic, singly ionized barium that can be used in a cryogenic liquid, a gaseous environment, and in vacuum. Such a source is necessary for the research and development (R and D) efforts of the Enriched Xenon Observatory (EXO). The EXO collaboration is planning a series of experiments designed to determine the mass of the neutrino by searching for the neutrinoless double-beta decay[3] of ^{136}Xe. To suppress possible radioactive backgrounds, EXO plans to add to the standard low background techniques that are customary in these experiments the ability to tag the barium daughter of the double-beta decay using resonant fluorescence.[4–6] Since possible detector technologies would include xenon time projection chambers in high pressure gas[4] or liquid[7] phase, the R and D work on Ba-tagging requires a method of releasing Ba^+ in such media. The injection through a thin window of Ba ions produced in an accelerator would clearly be possible but it would require expensive equipment and would result in very highly ionized states, owing to the electron-stripping in the entrance window and in the high density medium.

The source presented here makes use of the Sm daughter of the decay

$$^{148}_{64}\mathrm{Gd} \rightarrow {}^{144}_{62}\mathrm{Sm} + \alpha \qquad (1)$$

to dislodge a Ba^+ ion from a BaF_2 layer coated over the Gd source. The α recoiling against the Sm is then detected in a semiconductor detector that is used as a substrate for the assembly, providing a tag for the ion emission. ^{148}Gd is a convenient α emitter because its half-life (74.6 yr) provides a good compromise between high specific activity and durability. In addition, the decay of ^{148}Gd is directly in the ground state of ^{144}Sm, so that no other radioactivity is produced.

[a)]Present address: Indiana University, Bloomington IN, USA.
[b)]Present address: University of Seoul, Seoul, Korea.

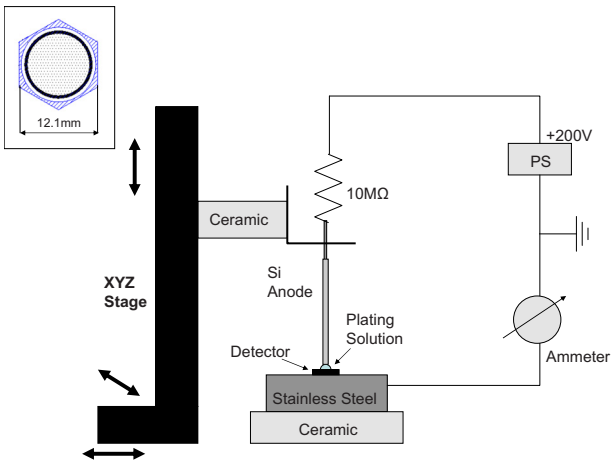

FIG. 1. (Color online) Schematic view of the radioactive Gd plating setup. The micrometers allow for an accurate and stable positioning of the anode ≃0.5 mm above the center of the detector being plated. A drawing of the Canberra PIPS® detector used is provided in the inset.

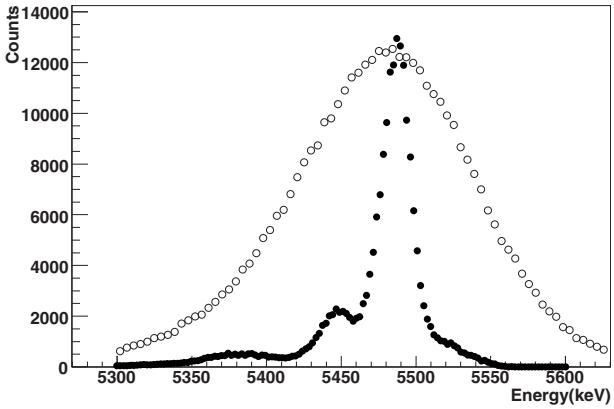

FIG. 2. α spectrum of an external ^{241}Am source recorded by the PIPS® detector before (full circles) and after (empty circles) the Gd plating. The three main α peaks at 5485.6, 5442.8, and 5388.2 keV are clearly distinguishable in the first data set. In this case the resolution of the 5485.6 keV peak is of 22 keV FWHM. After plating, the energy resolution degrades substantially and the new resolution of ~130 keV FWHM makes it impossible to resolve the three ^{241}Am lines.

Finally, Gd can be reliably electroplated in thin, uniform layers, as will be discussed.

The Gd source is deposited onto a PIPS® α detector[8] and a special technique is used to confine the activity to a small central region. A thin layer of BaF_2 is then vapor-deposited over the entire detector. The assembly is mounted in a custom metal-ceramic holder that is suitable for ultraclean operations and moderate vacuum bakeouts. The ion source obtained is inexpensive, compact, and suitable for a variety of environments. The selection of coatings other than BaF_2 can provide similar sources for most elements.

II. SOURCE FABRICATION

^{148}Gd is obtained in the form of $GdCl_3$ in HCl aqueous solution. Natural Gd is present as carrier in the solution in the approximate ratio[9] ^{nat}Gd:^{148}Gd=1:6.6×10^{-4}. Gd electroplating works best in isopropanol (IPA) from gadolinium nitrate.[10] So the chloride is transformed into nitrate as

$$GdCl_{3(aq)} + 3HNO_{3(aq)} \rightarrow Gd(NO_3)_{3(aq)} + 3HCl_{(aq)}. \quad (2)$$

The reaction is achieved by drying a 500 μl (0.1 μCi) $^{148}GdCl_3$ batch on a hot plate and adding 500 μl of 1M HNO_3.[11] The water is then evaporated again and more HNO_3 is added, repeating the process three times. After the last drying cycle, the $^{148}Gd(NO_3)_3$ is dissolved in 500 μl of IPA.[12] 25 μl of this solution are calculated to have an activity of 185 Bq. A measurement of the activity, performed by dissolving one 25 μl batch in a liquid scintillation counter,[13] confirms a carry-over efficiency of ~100%. Since the $Gd(NO_3)_3$ concentration is extremely low, a drop of 0.05M HNO_3 is added in 10 l of the IPA in order to increase the conductivity of the plating solution to an acceptable level.

The use of a conventional plating cell is excluded because of the requirement to deposit the ^{148}Gd only in a specific and small region of the detector. Therefore, a plating circuit is established by mounting a PIPS® detector on a horizontal support and lowering an anode to a position about 0.5 mm above the center of the detector using a micrometer, as shown in Fig. 1. Using a calibrated pipette a small drop of ~5 μl of solution is then deposited between the anode and the detector, which serves as the cathode in the circuit. The drop remains in place because of surface tension. A 200 V potential is then applied to the circuit via a 10 MΩ current-limiting resistor, establishing a current that is measured to be 18 μA. Depending on the activity required more 5 μl batches are added, as the solvent evaporates, for a total of 25–50 μl. Finally, pure IPA aliquots are added, again to counter evaporation. A total plating time of 15 min was found to be adequate by trial and error by measuring the activity on the detector (since the charge transport in the cell is completely dominated by the HNO_3 added to the IPA and has no relation with the amount of Gd deposited). Because of the nonradioactive Gd carrier, a source of ≃200 Bq activity, obtained from 25 μl plating solution, roughly covers a surface of 8×10^{-2} cm^2 with ~10 monolayers of Gd.

Initial tests using Pt anodes were found to produce large contaminations in the Gd coatings. This was evident by optical inspection of the plated detector. Such contaminations are unacceptable because they reduce the energy of the Sm recoils, as confirmed by the analysis of the α energy spectrum from the source measured in an external surface barrier detector. Anodes obtained using 4 mm wide slices of a B-doped silicon wafer (resistivity ≃50 Ω m) were found to be sufficiently clean and were used for the work presented here.

The α detector used as a substrate has surface contacts formed by shallow ion implantation and it is especially appropriate because of its ruggedness. Its hexagonal shape (also shown in Fig. 1) is of no particular significance here. The functionality of the detector after plating and the quality of the plated source are verified by α-counting both with the source-substrate detector ("self-counting") and, in some cases, with an external surface-barrier detector[14] in a vacuum chamber. In addition, an external ^{241}Am source is used to verify the detector performance and resolution after plating. A typical ^{241}Am spectrum recorded by the PIPS® detector with a 50 V bias and 2 μs shaping time, before and after Gd plating is shown in Fig. 2. The three peaks at 5485.6, 5442.8,

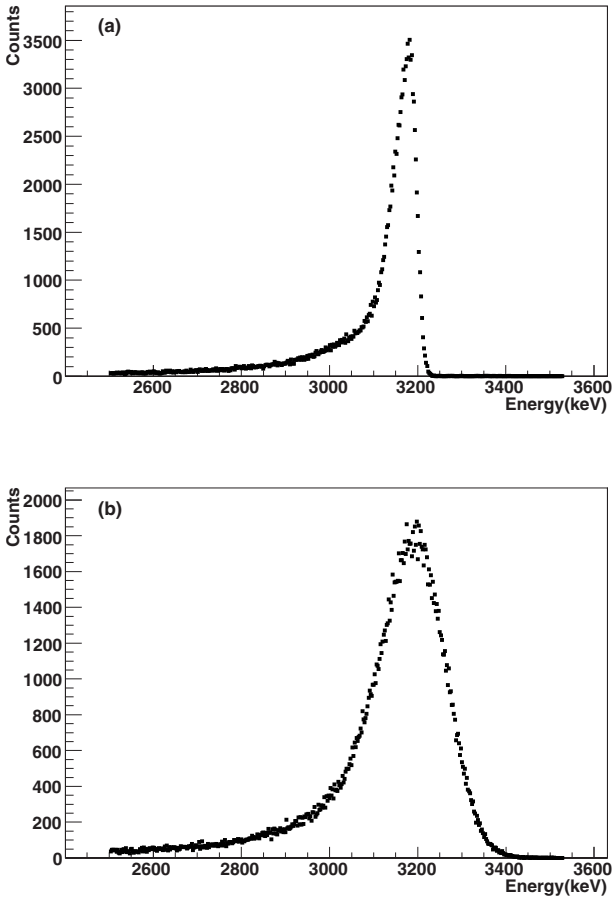

FIG. 3. ^{148}Gd "self-counted" α spectra. Panel (a) shows the spectrum of the ^{148}Gd layer only. The FWHM energy resolution is ~60 keV. Panel (b) shows the spectrum after 40 nm of BaF_2 are deposited over the source. The FWHM energy resolution is in this case ~170 keV.

and 5388.2 keV are clearly visible before plating, with a 22 keV full width at half maximum (FWHM) resolution for the most prominent peak. This is somewhat worse than the 14 keV FWHM stated by the manufacturer. The spectrum after Gd plating is substantially broader (~130 keV FWHM), presumably due to some deterioration of the detector and some energy loss in the Gd and other impurities left on the surface by the plating process. This degradation, however, appears to be stable in time and is not important for the simple α detection required in tagging the ion emission. The spectrum from the single 3182.7 keV α emitted by the ^{148}Gd plated on a detector shows [Fig. 3(a)] a resolution of ~60 keV FWHM.

The activity of the plated ^{148}Gd is measured by reading out the signal from the α detector, as will be described in the next section. For typical sources this activity is ≃200 Bq and matches, within experimental uncertainties, the activity measured in the plating solution, implying that the plating efficiency is rather high.

A coating of the appropriate chemical species and thickness will generally produce free ions and neutral atoms dislodged by the collision of the 89 keV recoiling ^{144}Sm. This is expected to be true for most elements, although with varying efficiencies, mainly due to the ratio of masses between the Sm and the "target" species. Different (in particular, heavier)

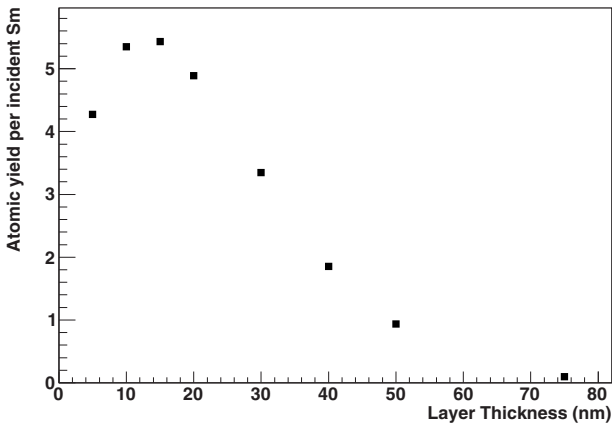

FIG. 4. Yield for Ba atoms as a function of layer thicknesses, as calculated by a SRIM simulation. Since SRIM does not distinguish between different charge states the yield from the graph includes neutral atoms, singly charged ions, as well as ions with a higher ionization state.

α emitters (e.g., ^{208}Po or ^{209}Po) could replace the ^{148}Gd, although this was not attempted in our work.

BaF_2 was chosen as the chemical species containing Ba because of its relatively good stability in air[15] and the fact that the other atomic species, fluorine, has a mass that is very different from that of Ba. The optimal layer thickness is estimated using the SRIM (Ref. 16) simulation package with full damage cascades simulation. Figure 4 shows the predicted Ba yields as a function of thickness. BaF_2 was simulated by simply providing SRIM with the appropriate number densities of Ba and F. Yields greater than one, such as those reported in Fig. 4, are not unusual in sputtering processes.

While the Ba yield can be larger than 1, as in the case of sputtering, it should be kept in mind that SRIM does not distinguish between neutral atoms and ions in different charge states, so that the yield of Ba^+ is not known from the simulation. The energy spectrum for Ba is predicted by SRIM to be peaked at zero with a long tail extending above 100 eV. 15 nm was chosen as the optimal layer thickness for the BaF_2, although some early sources were fabricated with thicknesses from 8 to 40 nm.

As already mentioned, electroplating was chosen as the technique to deposit the α emitter because of the layer quality and the possibility of obtaining deposits that are easily limited to a specific area. The technology for the overcoating by the target species was then chosen so as not to chemically interfere with the radionuclide and, at the same time, provide a uniform layer over the entire front surface of the detector. Vacuum evaporation is suitable for this since the energy of the ions is low (compared to sputtering) and no wet chemistry is involved. In our system, tantalum boats are ohmically heated to an appropriate temperature and the thickness of the deposited layer is monitored by a microbalance located next to the source being plated. Most materials can be deposited in this way or using electron-beam heating for refractory materials. As shown in Fig. 3(b), the α energy resolution from the ^{148}Gd source is further deteriorated after the BaF_2 coating. While the origin of the deterioration is not understood, the detector is still functional and completely adequate to tag the decay and the subsequent emission. In order to

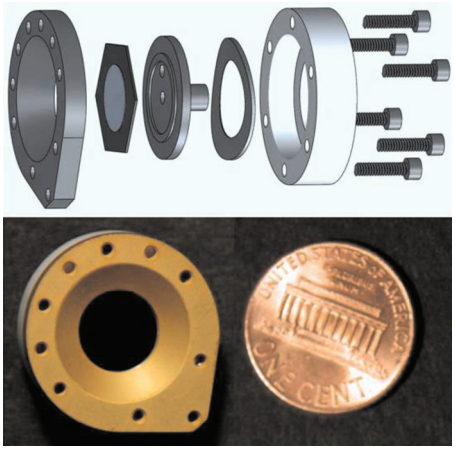

FIG. 5. (Color) Top: Exploded view of an ion source in its metal-ceramic ultrahigh vacuum mount. The "wavy washer" provides a uniform force on the detector to ensure proper contact. All metallic parts are made out of gold-plated stainless steel. The ring to the right of the drawing is made out of Macor®. Bottom: Photograph of a completed source.

ensure the best possible purity for the BaF_2 coating, a small scintillation-grade BaF_2 crystal[17] was used in the evaporation process.

Sources prepared as described above are then mounted in the special holders shown in Fig. 5. All metallic parts are made of gold-plated stainless steel, and the insulating ring separating the two diode contacts is made out of Macor®. The elastomer used in the standard encapsulation to maintain a constant pressure on the contacts is replaced by a gold-plated wavy washer. The holders allow for cooldown to 77 K and are compatible with the extreme cleanliness required for ultrahigh vacuum operations as well as for operation in liquefied noble gases (in particular liquid xenon).

III. SOURCE CHARACTERIZATION

The ion emission from the source is analyzed with a simple time of flight (TOF) spectrometer comprising two Einzel lenses and designed to maximize the transport efficiency of ions from the rather large emittance produced by the source to a channel electron multiplier[18] (CEM). The spectrometer is designed with a central drift region and electrodes at the two ends that allow for the independent adjustment of the electric field at the surface of the source (E_{source}, 350 V/cm$<E_{source}<$750 V/cm) and the ion impact energy on the CEM (2400 eV$<K<$3800 eV). The overall length of $\simeq$17 cm produces a TOF for Ba^+ of $\sim$5 μs, depending on the exact configuration of potentials. The "start" signal for the TOF measurement is provided by the PIPS® detector on which the source is built and the "stop" is provided by the CEM pulse. In this case the 45 V bias of the PIPS® detector is provided by a battery, so that the entire source can be floated to high voltage as required by the different configurations of the spectrometer. Both signals from the source and the CEM are digitized with flash analog-to-digital convertor (ADCs) (FADCs) at 250 MS/s. The signal from the source is used to trigger an acquisition. While a fast preamplifier is used for the CEM pulse, the signal from the source is fed into an Ortec model 142 preamplifier, Oak Ridge, TN, USA, followed by a model 474 timing filter amplifier with 100 ns shaping. Timing thresholds are applied offline.

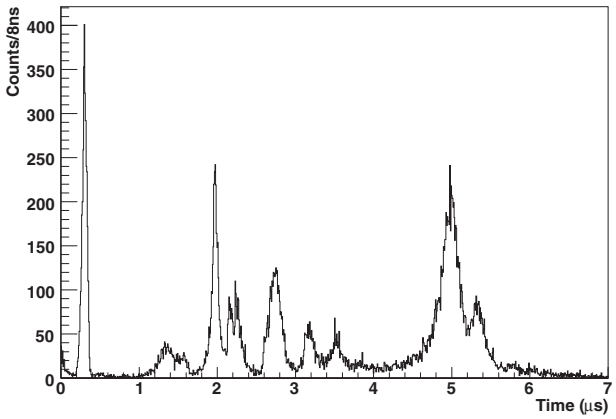

FIG. 6. TOF spectrum for a typical Ba source. The source has a measured ^{148}Gd activity of 173 Bq and a 15 nm thick BaF_2 coating. The Ba^+ yield, measured as the integral of the main peak, is of 2.7 Hz.

A typical TOF spectrum obtained for the intermediate values of E_{source}=550 V/cm and K=2800 eV is shown in Fig. 6. The prominent peak around 5 μs has a position and width consistent with those predicted by a SIMION (Ref. 19) simulation for Ba^+ ions. Such simulation includes the correct natural isotopic mix for the atomic mass of Ba and an initial energy distribution derived by the SRIM output, as explained below. A fit of this peak to five Gaussian functions representing the main Ba isotope masses provides an estimate for the spectrometer FWHM resolution of 5.8 amu at $\simeq$137 amu. The assignment of the peak to Ba^+ is corroborated by the observation that no such peak is present in a source where the BaF_2 coating is replaced by Al. In addition, and maybe most importantly, Ba deposited from a source of this type onto a clean silicon substrate was then desorbed and resonantly ionized with two lasers. From this very specific result it is clear that positive Ba ions are indeed emitted by the source.

According to SRIM the energy spectrum of the Ba emitted by the source peaks at zero and decreases monotonically, with 17% of the spectrum having energies greater than 300 eV. Since, as already mentioned, the SRIM simulation is unable to distinguish between neutral and charged states, a different method is required to estimate the expected ion fraction, $\alpha=n_+/n_{total}$. Ideally this ratio would be known as a function of Ba energy. Unfortunately, a general understanding of the ion fraction in sputtering is still an open question, even for pure metals, and data are completely lacking for ionic compounds, such as BaF_2.[20] Some models and experimental data describe α by a decaying exponential in the inverse velocity plus a constant term, with the transition taking place around a critical velocity of $\sim$2 cm/μs.[20] The net result of this function combined with the sputtering energy distribution is that the fraction of ions is low at low energy and approaches unity at higher energy. The transition takes place around 2 cm/μs, or $\sim$300 eV in the case of Ba.

The actual energy distribution of Ba^+ ions affects the

TABLE I. Possible assignment of the TOF peaks for the source in Fig. 6. The associations of H^+ and Ba^+ (in italics) are assumed and used to compute the mass values for the other peaks.

Time (μs)	Measured mass (amu)	Possible assignment (known mass in [ ])
0.31	*1.01*	H^+ *[1.01]*
1.44	12.9	C^+ [12.0]
1.99	23.5	Na^+ [23.0]
2.16	27.6	Si^+ [28.1]
2.23	29.3	⋯
2.75	43.5	$C_2H_5O^+$ [45.1]
3.19	57.9	$C_3H_8O^+$ [60.1]
3.55	70.9	Ba^{2+} [68.7]
4.99	*137.3*	Ba^+ *[137.3]*
5.33	156.2	BaF^+ [156.3]

transport efficiency of the spectrometer significantly. While such efficiency is calculated to be 85% for the entire energy distribution produced by SRIM, it is only 8% for the part of such energy distribution exceeding 300 eV. Also the TOF peak position and width are to some extent predicted to vary for different regions of the emittance of the source. A simple consistency check for the Ba^+ yield can be made by assuming in the simulation that only ions (neutrals) are produced above (below) a certain energy cutoff. The yield, TOF peak position, and width are then compared with data for a variety of values of E_{source} and K. A reasonably good description of the data occurs for a 300 eV cutoff. The simulated rate reproduces the data within a factor of 2 when E_{source} and K are varied from 550 V/cm and 2800 eV to the extremes mentioned above. With the same cutoff value the simulation also provides a good prediction for the Ba^+ TOF peak position (better than 10%) and width (better than 25%), again when scanning E_{source} and K from their central values to the extremes.

For the spectrum in Fig. 6 the Ba^+ yield is measured to be 2.7 Hz. Using the α activity of 173 Bq, SRIM predicts a rate of Ba emission of 430 Hz for the 15 nm thick BaF_2 coating (see Fig. 4). Assuming that the ions comprise only those Ba atoms ejected with energy above 300 eV, or, according to SRIM 17% of the total, the Ba^+ emission rate is calculated to be 73 Hz. Using the spectrometer efficiency of 8% appropriate for this energy range, a rate of 5.8 Hz is predicted to arrive at the CEM. The ratio between this figure and the measured rate of 2.7 Hz is consistent with typical CEM efficiencies for ions with the velocities expected here.

The TOF spectrum for light masses is similar to the one observed for the source coated with Al. Its interpretation nevertheless poses some challenges because of the limited resolution of the spectrometer, the large emittance of the source, and the difficulty in predicting the charge to neutral ratio as a function of the species and initial energy. A possible assignment, obtained using as reference the Ba^+ peak and the peak at 0.31 μs, assuming to be due to H^+ is shown in Table I. The presence of a prominent Na^+ peak is not surprising, given the common presence of sodium contamination on surfaces. Emission of some Si from the substrate is not unexpected, while $C_2H_5O^+$ and $C_3H_8O^+$ are commonly observed in mass spectra of the IPA that is used in the Gd plating process. No compelling assignment is available for the peak at 2.23 μs. Finally, the satellite peak at a mass larger than that of Ba is not present in the Al coated source and it may be attributed to BaF^+.

IV. CONCLUSIONS

We have built a simple, inexpensive, and compact source of single Ba^+ ions using the recoils of an α emitting radionuclide to dislodge Ba atoms from a BaF_2 coating. The source uses a surface barrier detector as a substrate, so that a tag is provided for the ion emission. Its simplicity and the possibility of delivering tagged ions in various environments make it attractive in applications where a low rate of individual ions is desirable. In addition the emission of neutral Ba, not useful for our purposes, may find other applications. The replacement of the BaF_2 with other materials provides the means of emitting ions from a large number of different species.

ACKNOWLEDGMENTS

We would like to thank K. Moody (LLNL) and L. Moretto (UC Berkeley and LBNL) for their radiochemistry advice. The support from the staff of the Stanford Health Physics group and, in particular, of D. Menke, is also gratefully acknowledged. We are also indebted to H. Newman and R-Y. Zhu (Caltech) for providing a high quality crystal of barium fluoride. Finally, we would like to thank Canberra Semiconductor NV and, in particular, M. Morelle for advice and for providing us with unencapsulated samples of their detectors used for practicing the different processing steps. This work was supported in part by NSF grant PHY-0652416.

[1] L. Valyi, *Atom and Ion Sources* (Wiley, London, 1977).
[2] *Handbook of Ion Sources*, edited by B. Wolf (CRC, Boca Raton, 1995).
[3] F. T. Avignone III, S. R. Elliott, and J. Engel, Rev. Mod. Phys. **80**, 481 (2008).
[4] M. Danilov *et al.*, Phys. Lett. B **480**, 12 (2000).
[5] B. Flatt *et al.*, Nucl. Instrum. Methods Phys. Res. A **578**, 399 (2007).
[6] M. Green *et al.*, Phys. Rev. A **76**, 023404 (2007).
[7] E. Conti *et al.*, Phys. Rev. B **68**, 054201 (2003).
[8] Model PD50 50 mm^2 active area unmounted wafer, Canberra, Meriden, CT.
[9] Eckert & Ziegler Isotope Products (private communication).
[10] K. Moody (private communication).
[11] TraceMetal grade, Fisher Chemical, Pittsburgh, PA.
[12] LC-MS Chromasolv® >99.9% grade, Sigma-Aldrich, St. Louis, MO.
[13] Measurement performed by the Stanford Health Physics Department, Stanford, CA.
[14] Model BU-014–050–100, Ortec, Oak Ridge, TN.
[15] *CRC Handbook of Chemistry and Physics*, 56th ed., edited by R. Weast (CRC, Boca Raton, 1975), pp. B-74–B-76.
[16] J.F. Ziegler, J.P. Biersack and M.D. Ziegler, *SRIM, The Stopping and Range of Ions in Matter* (Lulu, Morrisville, 2008).
[17] Produced by the Beijing Glass Research Institute, Beijing, China.
[18] Model 2403, DeTech, Palmer, MA.
[19] See http://www.simion.com for a description of this electrostatic lens design and analysis package.
[20] A. Wucher, Appl. Surf. Sci. **255**, 1194 (2008).